Ocean Dynamics (2011) 61:1981–1994
DOI 10.1007/s10236-011-0464-x

Autonomous underwater vehicle teams for adaptive ocean sampling: a data-driven approach

Andrea Munafò · Enrico Simetti · Alessio Turetta · Andrea Caiti · Giuseppe Casalino

Received: 15 January 2011 / Accepted: 20 June 2011 / Published online: 10 July 2011

Abstract The current technological developments in autonomous underwater vehicles (AUVs) and underwater communication have nowadays allowed to push the original idea of autonomous ocean sampling network even further, with the possibility of using each agent of the network not only as an operative component driven by external commands (model-driven) but as a reactive element able to act in response to changing conditions as measured during the exploration (data-driven). With this paper, we propose a novel data-driven algorithm for AUVs team for adaptive sampling of oceanic regions, where each agent shares its knowledge of the environment with its teammates and autonomously takes decision in order to reconstruct the desired oceanic field. In particular, sampling point selection is made in order to minimize the uncertainty in the estimated field while keeping communication contact with the rest of the team and avoiding to repeatedly sampling sub-regions already explored. The proposed approach is based on the use of the emergent behaviour technique and on the use of artificial potential functions (interest functions) to achieve the desired goal at the end of the mission. In this way, there is no explicit minimization of a cost functional at each decision step. The oceanic field is reconstructed by the application of radial basis functions interpolation of irregularly spaced data. A simulative example for the estimation of a salinity field with sea data obtained using the Mediterranean Sea Forecasting System is shown in the paper, in order to investigate the effect of the different uncertainty sources, including sea currents, on the behaviour of the exploration team and ultimately on the reconstruction of the salinity field.

Keywords Autonomous underwater vehicles (AUVs) · Vehicles cooperation · Data-driven approach · Ocean sampling · Autonomous ocean sampling networks

Responsible Editor: Michel Rixen

This article is part of the Topical Collection on *Maritime Rapid Environmental Assessment*

A. Munafò (✉)
Inter-university Center on Integrated Systems for the Marine Environment, Centro E. Piaggio, University of Pisa,
Largo L. Lazzarino, 1,
56122 Pisa, Italy
e-mail: andrea.munafo@dsea.unipi.it

E. Simetti · A. Turetta · G. Casalino
Inter-university Center on Integrated Systems for the Marine Environment, Department of Communication,
Computer and System Sciences, University of Genoa,
Via Opera Pia 13,
16145 Genoa, Italy

E. Simetti
e-mail: simetti@dist.unige.it

A. Turetta
e-mail: turetta@dist.unige.it

G. Casalino
e-mail: casalino@dist.unige.it

A. Caiti
Inter-university Center on Integrated Systems for the Marine Environment, Centro E. Piaggio, University of Pisa,
Largo L. Lazzarino, 1,
56127 Pisa, Italy
e-mail: andrea.caiti@dsea.unipi.it

1 Introduction

Ocean monitoring and exploration operations for oceanographic, biological and geophysical purposes have always

been costly and time-consuming. Recent technological developments have suggested a possible solution to these traditional limitations, proposing new approaches, based on the use of autonomous underwater vehicles (AUVs).

In the early 1990s, thanks to the fast development of autonomous oceanographic instrumentation and related communication systems, Curtin et al. (1993) have promoted the vision of Autonomous Ocean Sampling Networks (AOSN); a highly integrated system of autonomous units, able to provide synoptic data repeatable over time in a cost-effective way.

The key idea of AOSN is to integrate a suite of fixed sensors with autonomous robotic vehicles, the AUVs, each one carrying some appropriate payload, and collecting data over appropriate survey tracks not reached by the fixed stations.

The critical component of the AOSN concept was the AUV, through which synoptic observations can be obtained at potentially very reduced cost. Moreover, the mobility of AUV can be exploited to improve forecasting, by merging observations with advanced ocean models: all the information gathered by the operational instrumentation is relayed to shore (or to a surface station) where it is integrated with now-casting–forecasting oceanographic systems (data assimilation). Moreover, the spatial uncertainty in the resulting forecast can be used to plan future AUV trajectories, in order to reduce such uncertainty (model-driven adaptive sampling).

At the time of the AOSN proposal, the available operational AUVs were designed for deep-water geophysical surveys, accordingly to the needs of the oil and offshore industries. However, advances in miniaturization and embedded systems technology has now made possible the design and realization of low-cost AUVs (Anderson and Crowell 2005; Alvarez et al. 2009) that, equipped with appropriate oceanographic payloads, can act as a team in mapping specific areas of the ocean.

In particular, the current technological development of underwater vehicles is driving the AOSN vision even further. While the presence of AUVs was seen at that time as simple operating units at sea, with the task of executing a mission generated remotely by the use of ocean models, the technical maturity of such devices makes it possible, nowadays, to delegate to the robotic systems at sea more complex tasks. For instance, on the basis of the data measured along the mission, a vehicle can modify its mission plan, without the need of supervision from a remote station. The key idea is that each AUV acts as a component of a team, sharing its information directly with its teammates so that at the end of the mission a common goal can be reached. In this context, the idea of AOSN can be widened from that of a *model-driven* network of autonomous sensors, in which the presence of an external supervisor and mission planner (the models themselves) is essential for the coordination of the whole set of vehicles, to a *data-driven* network of agents in which each robot acts in cooperation with the rest of the network with which it shares some common knowledge/data and that allows the network as a whole to move in accordance to some desired mission objective, in response to change in the data measured by the various components. This approach should not be considered an alternative to model-driven adaptive sampling, but in fact a complementary approach that may come effective in all the situations whenever availability of model predictions is limited either by communication constraints or by the model capabilities themselves.

Several cooperation and coordination algorithms for mobile robotic vehicles in the model-driven approach (Yilmaz et al. 2008) have been successfully applied to AUV teams and oceanographic gliders (Paley et al. 2008) and some large-scale experimentation, in which networks of mobile and fixed sensors, autonomous or semi-autonomous, have been employed to monitor the evolution of ocean dynamics, have been successfully reported (Curtin and Bellingham 2009). One recent very interesting work, in the field of coordination of autonomous gliders, is the one reported in Leonard et al. (2010). In this work, a fleet of gliders is coordinated in order to optimize sampling patterns accordingly to the on-line measured speed, which depends on the local oceanographic conditions; this is done in conjunction with trajectory planning based on data assimilation and ocean model predictions.. The experiment described shows an instance where model-based adaptive sampling is coupled to data-driven adaptation.

Nevertheless, the challenges posed by the ocean environments are such that there are still scientific and technological problems to be solved for the realization of the AOSN vision, and in particular for data-driven adaptive sampling. One challenge to be solved is related to the problem of underwater communication among the underwater platforms either fixed or mobile that compose the network: acoustic communications cannot be always guaranteed and are strongly dependent on environmental conditions of the mission area.

Within this paper, we propose a novel algorithm for the cooperation and coordination of a team of AUVs in an environmental mapping mission within the data-driven paradigm of uncertainty management. Each agent shares its knowledge with the rest of the team, and it is able to adapt its behaviour to the conditions encountered during the exploration. Specifically, the team explores the area with the aim of maintaining a desired accuracy on the reconstruction of the environmental map through the estimation of the local smoothness properties of the map itself. In addition, while guaranteeing the accuracy of the environmental field, the cooperation algorithm ensures that each vehicle keeps communication with the other agents while maximizing the local distance among the AUVs. The methodology for estimating the oceanographic property of a given area is based on the approximating properties of

radial basis functions (RBFs). This approach has been linked to AUV team cooperation and adaptive ocean sampling by Caiti et al. (2007). Strategies for application of the RBFs-based adaptive sampling by team cooperation with communication constraints have been proposed in Alvarez et al. (2009), where a serial graph structure with hierarchical ordering of the vehicles in the team was introduced. The hierarchical, graph-based structure had the theoretical advantage of making it possible to apply the well-known dynamic programming algorithm in a distributed way in order to optimize the efficiency of the exploration (i.e. the overall number of sampling stations) while preserving the inter-vehicle communication constraints. This approach however has the disadvantage of being fragile with respect to loss of communication among the vehicles, eventually leading to a disruption of the graph structure itself. Moreover, a relatively heavy burden in terms of communication among the vehicles is required each time a new sampling measurement is made available: in particular, the team has to communicate in ordered sequence twice along the serial graph, in correspondence of the forward and backward phase of the dynamic programming algorithm. Alvarez et al. (2009) proposed also a different algorithm, more robust with respect to the dynamic programming one, at the price of an increased local computational burden and of much heavier requirements in inter-vehicle communications.

While the approaches of Alvarez et al. (2009) have the merit of providing a theoretical justification of the global optimality of the algorithms proposed, the constraints in terms of communications, computational overload, and fragility with respect to the loss of the graph structure represent non negligible drawbacks in practical implementations. In this paper, we introduce a heuristic algorithm in which each vehicle in the team adapts its sampling strategy based on simple local rules that take into account the available information as received by the vehicles within communication range. While the local rules have been designed in order to maintain communication contact among the vehicles, sudden loss of inter-vehicle communication reduces the efficiency of the sampling task but does not disrupt it, providing a gentle degradation of the algorithm. Moreover, when the loss of communication is intermittent, as it is often the case in underwater communication channels, the algorithm is able to accommodate for it in a seamless way, without need of additional computation or rescheduling of the communication hierarchy. In fact, the underlying communication scheme can just be as a simple broadcast from each vehicle in a Time Division Multiplex scheme with repeaters, although more elaborate networked communication schemes are certainly not to be ruled out. The price paid by the "local rules" approach is that a formal justification of the global optimality of the algorithm is now lacking, since the global performance becomes an effect of the emergent behaviour of the team and not of a pre-programmed effort. Simulative comparisons with the results of the previously defined optimal graph-based algorithms show that indeed the algorithm presented here has only a slightly worse performance, in terms of required number of sampling stations. We think it very interesting, and indeed a needed step-ahead, that optimality can be approximated by a truly locally distributed cooperation approach, much easier to implement in practice.

The proposed method is described as a stand-alone data-driven approach. No integration with model-driven prior information is considered for clarity of the presentation. However, the method can be embedded into a wider model-driven scheme in a number of different ways and it is clear that the integration of the two approaches is likely to give the most benefit in operational applications.

The paper is organized as follows: in the next section, the problem setting and the general cooperative approach is described. In Section 3, we go into the details of the proposed cooperative adaptive algorithm for AUVs team. Results from simulative testing of the approach in realistic environments are shown in Section 4, and conclusions are summarized in Section 5. Finally, in the Appendix, we provide details on the approximating properties of RBFs, linking their usage to the proposed sampling method.

2 Problem statement and cooperative approach

It is assumed that estimation of oceanographic field is carried out exploiting the RBFs approach on irregularly sampled data set (Caiti et al. 2007). We do not go into the detail of the approximation properties of RBFs since it would go beyond the scope of this paper, but we refer the interested reader to the Appendix and to Schaback (1995, 1997) and Iske (2003). We wish to underline that the approach is deterministic, i.e. it assumes a deterministic field to be approximated everywhere from a knowledge of a sparse set of data points.

This approach, at least in the form presented here, requires that the oceanographic field does not change in time within the mission period. Fluctuations in time and space within this period are smoothed out by the RBF method as high-frequency disturbances. Considering that the mission period itself may vary according to vehicle speed and extension of the area of interest this implies that the scale of the above mentioned high-frequency disturbances is not absolute but related to the mission characteristics. For instance, the longer the mission time, the lower the frequencies of the field that will be recovered by the method. It is clear that with current available technology this assumption is better justified in limited areas like coastal waters as opposed to open oceans, long-term

operations. Case by case analysis has to be carried out in order to quantitatively determine a priori the high-frequency components of the oceanic field that will be missed by the proposed method.

In the following, we treat all the quantities as deterministic, as routinely done in the RBFs literature.

Let us suppose we have the availability of n AUVs, each one equipped with a sensor able to point-wise sample an environmental quantity θ at the geographical coordinates $\mathbf{x} = (x, y)$ and with an acoustic modem for communication characterized by a maximum range R_C. The communication performance can be set based on measurements from on-board sensors (Caiti et al. 2009). Note that the quantity θ will usually be measured at position x as a function of depth, i.e., at each sampling station a depth profile of θ will be measured. While the RBF approximation and the cooperation algorithm can deal without modification with 3-D oceanic fields, in the following we omit the dependence of θ from depth for notation simplicity. Also, in the simulated examples, we report 2-D field approximation to make it easier to evaluate the main merits and drawbacks of the proposed method. Note finally that the assumed modality of operation for each AUV is that of moving from one sampling station to the next, and collecting data (depth profiles) only at the sampling station, i.e. the vehicles do not record data when on transit between stations. While this modality of operation is justified by the technical characteristics of some AUV class (Alvarez et al. 2009), other modalities could be considered. We refer the reader to Section 5 for some more observations on this point.

We consider a sampling of the area occurring at incremental stages: stage 1 corresponds to the first n sampling points in the area (i.e. the coordinates at which each vehicle has taken its first sample), stage 2 to the second set of n sampling points, etc.

Let $\mathbf{x}_k^{(j)}$ be the position of the sampling point of vehicle j at stage k; we are interested in determining the position of the sampling points of each vehicle at the next stage $k+1$. We want to determine these points fulfilling the following qualitative objectives:

(a) Increase sampling point density in the areas poorly covered by previous sampling points;
(b) Spread the vehicles around the area in order to cover it with the minimum number of sampling points;
(c) Maintain control of the accuracy with which the oceanic field will be approximated;
(d) Maintain communication among the vehicles;

Let $M_k = \bigcup_{j=1}^{n} \bigcup_{i=1}^{k} \mathbf{x}_i^{(j)}$ be the set of points sampled by the whole team and known after measurement stage k. Let us define the set $I_k = \{M_k; \theta = \theta(\mathbf{x}), \mathbf{x} \in M_k\}$ as the information set available after stage k. Let S be an approximation algorithm that computes a deterministic estimate $\widehat{\theta}$ of the quantity θ over the whole region A on the basis of the available information $I_k : \widehat{\theta}_{I_k}(\mathbf{x}) = S(I_k)$. In our case, the approximation algorithm S is built through RBFs as described in the Appendix. On the basis of the approximation algorithm S and the available information set, the estimation error (1) is defined as:

$$\varepsilon_k = \left\| \theta(\mathbf{x}) - \widehat{\theta}_{I_k}(\mathbf{x}) \right\| \tag{1}$$

We furthermore assume (as it is the case with RBFs schemes) that, given an approximated map $\widehat{\theta}_{I_k}$, defined over the whole region A of interest, the approximation algorithm gives a prediction $\widehat{\varepsilon}_k$ of the estimation error (1) at any point in the region A; the predicted estimation error is minimum at the sampled point, and it monotonically increases as the distance of a generic point x increases from the set M_k. The distance of x from M_k is defined as $d(\mathbf{x}, M_k) = \inf_{\mathbf{x}_i \in M_k} \|\mathbf{x} - \mathbf{x}_i\|$. Let us finally assume that the main mission goal is to survey the region so that, eventually, the estimation error (1) is everywhere below a desired threshold D. In order to incrementally sample the area, we want to choose the sampling position at stage $k+1$ of any vehicle j such that:

$$\min_{\left\{\mathbf{x}_{k+1}^{(j)}\right\}_{j=1}^{n}} \sup_{\mathbf{x} \in A} d\left(\mathbf{x}, M_k \cup \left\{\mathbf{x}_{k+1}^{(j)}\right\}_{j=1}^{n}\right) \tag{2a}$$

$$\max_{\left\{\mathbf{x}_{k+1}^{(j)}\right\}_{j=1}^{n}} \text{convex hull}\left(M_k \cup \left\{\mathbf{x}_{k+1}^{(j)}\right\}_{j=1}^{n}\right) \tag{2b}$$

for any j

$$\widehat{\varepsilon}\left(\mathbf{x}_{k+1}^{(j)}\right) \le D \tag{2c}$$

there is at least one ordered path 1, 2, …, j, $j+1$, …, n such that

$$\left\|\mathbf{x}_{k+1}^{(j)} - \mathbf{x}_{k+1}^{(j+1)}\right\| \le R_C^{(j)}, \left\|\mathbf{x}_{k+1}^{(j)} - \mathbf{x}_{k+1}^{(j-1)}\right\| \le R_C^{(j)} \text{ for any } j \tag{2d}$$

The problem stated by Eq. 2 is a multi-objective constrained optimization problem. Note that the Eqs. 2a, 2b, 2c, 2d corresponds to the formal statement of the qualitative objectives (a), (b), (c), (d) as stated before. The above formulation refers to a sampling strategy based on synchronous incremental stages with complete information available to all the vehicles through complete network connectivity. In the distributed cooperative algorithm formulation in Section 3 the synchronous assumption, as well as the assumption of complete network connectivity and information availability will be relaxed, and in fact the motion rules described in Section 3 can be applied without modification also in asynchronous way and with a partial local knowledge of the information set, resulting from

incomplete communication. It is clear, however, that with incomplete information, degradation on the performance, and hence sub-optimality with respect to Eq. 2, will be obtained.

The mission scenario to which the proposed algorithm is best suited is that of missions requiring sampling of a given quantity (e.g., salinity or temperature) at a specific geographical location. This means that the overall mission time must be smaller than the time constant of the oceanic process observed.

Let us suppose the vehicles have an initial configuration such that the communication constraints are satisfied. As soon as the jth agent executes its kth sampling measurement and communicates it to the reminder of the team, the information set I_k becomes available and it is used by each agent to compute its exploring radius $\rho_{k+1}^{(j)}$. The exploring radius (see Fig. 1), which coincides with the radius of the circumference of the circle centred in the last sampling point $\mathbf{x}_k^{(j)}$, represents the maximum range, from the current sampling location, at which the next sampling station can be located maintaining the constraints on the predicted approximation error, i.e. $\widehat{\varepsilon}_k(\mathbf{x}) = D$ for any $\mathbf{x}$ s.t. $\left\|\mathbf{x}_k^{(j)} - \mathbf{x}\right\| = \rho_{k+1}^{(j)}$ (see the Appendix on how the exploring radius is computed in the case of RBFs approximation).

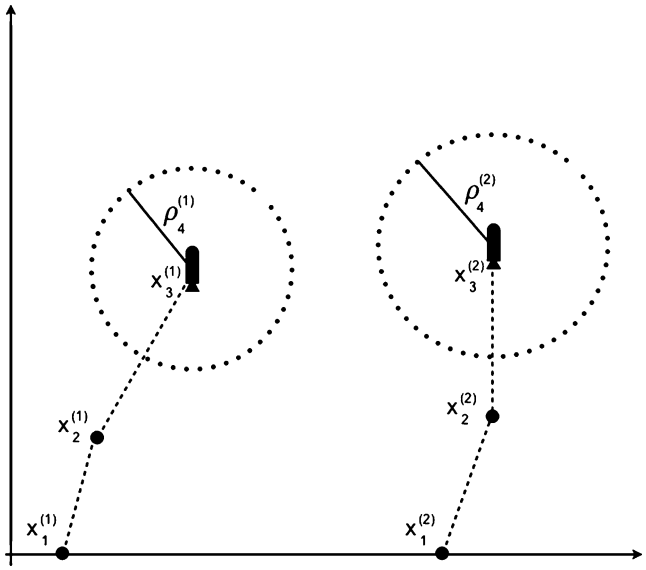

Fig. 1 Pictorial representation of an exploration step: after a new measurement is executed by one of the agents, it is communicated to the other agents and used by each vehicle to compute its exploring radius $\rho_{k+1}^{(j)}$. The exploring radius, which coincides with the radius of the circumference of the circle centred in the last sampling point $x_k^{(j)}$, represents the maximum range, from the current sampling location, at which the next sampling station can be located maintaining the constraints on the predicted approximation error (see Appendix on how this can computed in the case of RBFs). The next sampling station for each vehicle will hence be located on the circumference of such a circle, while its final location depends on the application of cooperation rules among the vehicles

Exploiting RBF properties, as described in Caiti et al. (2007) and references therein and as reported in the Appendix, makes it possible to approximate Eq. 1 as:

$$\varepsilon(\mathbf{x}) = |\theta(\mathbf{x}) - S(\mathbf{x})| \cong \|S(\mathbf{x})\|_{\phi} F_{\phi}\left(h_{\rho}(\mathbf{x})\right) \tag{3}$$

where $S(\mathbf{x})$ represents the RBF approximation of the environmental map, $\|\cdot\|_{\phi}$is the norm in the RBF native space which takes into account the smoothness of the estimated map, F_{ϕ} is the *spectral factor*, depending solely on the specific RBF choice (e.g. multiquadrics, gaussians, exponentials, etc.), and $h_{\rho}(\mathbf{x})$ is the *fill distance* representing the minimum distance among the samplings in the map and which, in the present context coincides with the exploration radius $\rho_{k+1}^{(j)}$. By evaluating Eq. 3 on the local approximation of θ, and solving the resulting nonlinear equation for the fill distance (see Appendix), each vehicle selects its exploring radius so that, at every point inside the circle, the error of the estimation map is below or equal to the required threshold. One critical factor in RBF theory is that the exploring radius will vary according to the variability of the approximated field. This means that the approximation scheme will automatically reduce the exploring radius in sub-areas where field variability is high and it will increase the exploring radius in sub-areas where field variability is low.

The selection of the specific point $\mathbf{x}_{k+1}^{(j)}$ in the circumference of centre $\mathbf{x}_k^{(j)}$ and radius $\rho_{k+1}^{(j)}$ does not affect the expected accuracy of the estimated field and it is used to satisfy the other mission objectives: (a) enforce the communication constraint among the vehicles, (b) spread the vehicles on the mission area to reduce the total mission time.

In the next paragraphs, we describe in detail the cooperative algorithm proposed, showing, through simulations, the performance in terms of sampling stations required, total mission time and approximation error of the reconstructed ocean field.

3 Cooperative adaptive algorithm description

Let us consider each vehicle motion described by the kinematical model:

$$\dot{\mathbf{x}}(t) = \mathbf{u}(t) + \mathbf{v}(t) \tag{4}$$

where $\mathbf{x} \in \Re^2$ is the robot position, $\underline{\mathbf{x}} \in \Re^2$ is the robot speed, $\mathbf{u} \in \Re^2$ is the control input to be defined, such that, at each time instant, the agent maintains the communication connectivity with at least one other agent in the team, and moves to minimize the approximation error of the oceanic

field, according to Eq. 2. Finally, the term $\mathbf{v} \in \Re^2$ allows for the inclusion of external motion disturbances acting on each agent as, for instance, marine currents.

In the following, we consider $R_C\left(j, \mathbf{x}^{(j)}, t\right)$ as the maximum communication range achieved by the vehicle j placed in $\mathbf{x}^{(j)}$ at time t, and $R_{\mathrm{MAX}}\left(j, \mathbf{x}^{(j)}, t\right), \forall j, \mathbf{x}, t$ as the maximum separation distance at which the jth vehicle wants to keep its closest neighbour. A vehicle has to be, at any time t, at a distance $d \leq R_C\left(j, \mathbf{x}^{(j)}, t\right)$ in order to receive data from vehicle j. These parameters are spatial dependent, and may vary with the position of the vehicle in the mission area.

The proposed cooperation algorithm defines each agent behaviour through simple rules, obtaining the overall mission goal as the result of the emergent behaviour of the team (Martinez et al. 2007; Tanner et al. 2003). Specifically, each vehicle, at each time instant, moves in accordance to the following three rules:

Rule 1 Go where sampling density is lower.
Rule 2 Move away from past measurements.
Rule 3 Move away from your closest neighbour, but without exiting from its communication radius.

The first two rules allow the robots to move towards unexplored zones of the area of interest, while the third rule modifies the team behaviour to maximize the distance between each other agent until the maximum distance allowed to maintain the communication is reached.

In addition, the vehicles interest in the specific rule is determined by a "function of interest" which regulates in which way the agent enforces the rule. A comparison among the functions of interest determines the priority of the rules followed at each time frame by each vehicle:

- The *attraction* function $h_A\left(\mathbf{x}_{fd}, \mathbf{x}^{(j)}\right)$ is a function of the agent's distance from the point $\mathbf{x}_{fd} \in A$, in the region A, whose distance from any other measurement point is the largest (see Fig. 2). It defines the interest in moving towards zone with lower density of samplings and it is used to apply Rule 1. Its parametric definition is:

$$h_A\left(\mathbf{x}_{fd}, \mathbf{x}^{(j)}\right) = \frac{\left\|\mathbf{x}_{fd} - \mathbf{x}^{(j)}\right\|_2^N}{N} \tag{5}$$

where N is a positive constant.

- The *avoid past measurements* $h_S\left(M_k, \mathbf{x}^{(j)}\right)$ function depends on the measurements set M_k available to vehicle j, on the current position of the vehicle $x^{(j)}$ and it is used to enforce Rule 2. In particular, the agent moves away from the past sampling locations with a direction that depends on the composition of each single repulsion force (see Fig. 3) generated by each point (see Fig. 4). It is defined as:

$$h_S\left(M_k, \mathbf{x}^{(j)}\right) = \sum_{h=1}^{n} \sum_{i=1}^{k_h} \frac{1}{\left\|\mathbf{x}_i^{(h)} - \mathbf{x}^{(j)}\right\|_2^p} \tag{6}$$

where p is a positive constant, $\mathbf{x}_i^{(h)} \in M_k$ is the position of the ith sampling point of vehicle h, *and* k_h is the number of samples taken by vehicle h.

- The *cooperation function* $h_C\left(\mathbf{x}^{(k)}, \mathbf{x}^{(j)}\right)$ depends on the current position of the agent $x^{(j)}$ and on the position of its closest neighbour $x^{(k)}$. It is used to enforce Rule 3 and it is modified on-line on the basis of the communication capabilities of the agent at a given spatial and temporal location. In accordance to the cooperation function (see Fig. 5), the vehicles separate themselves as much as they can while guaranteeing that the communication links are always active (defines the

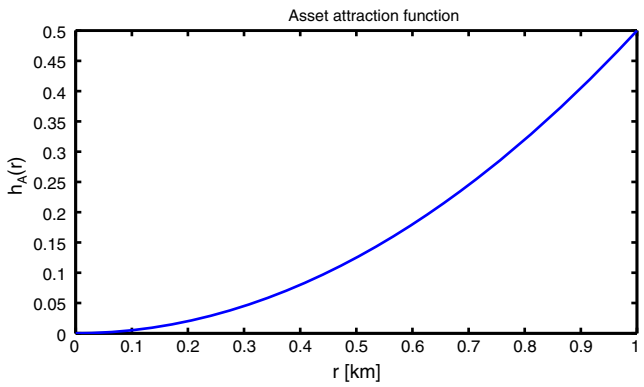

Fig. 2 Function of interest for Rule 1: move towards zone where the density of measures is lower. The higher the distance from the zone of interest the higher the interest in applying the rule

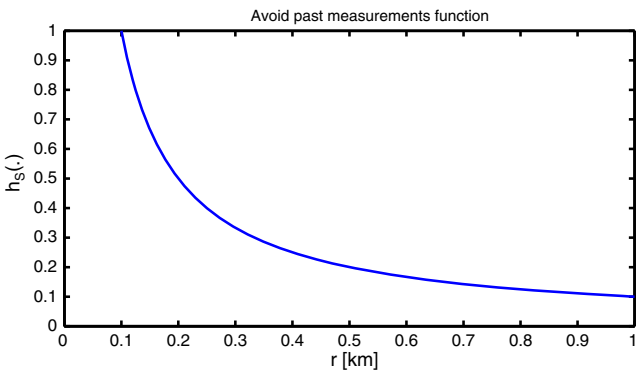

Fig. 3 Interest function for Rule 2 (move away from the past sampling points) as a function of the agent distance from one sampling station: the closer the vehicle is to a past sampling location the more it wants to move away from it

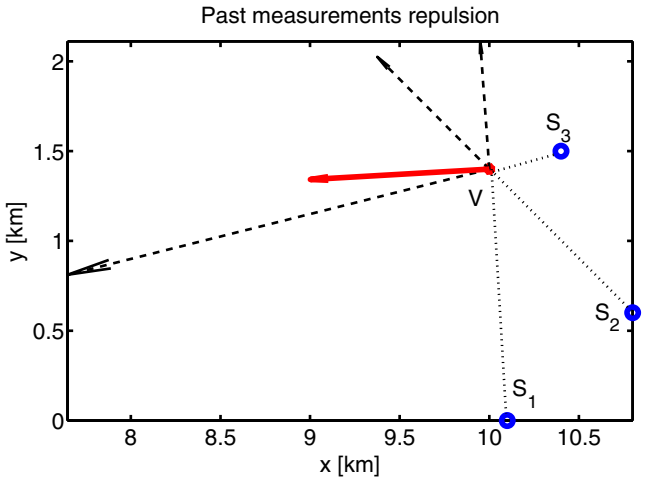

Fig. 4 Composition of past measurements (S_1, S_2, S_3) influence on the agent (marked as V in the picture). The agent final direction is indicated by the *solid-line arrow*

maximum separation between two vehicles). It is defined as:

$$h_C\left(\mathbf{x}^{(k)},\mathbf{x}^{(j)}\right) = \begin{cases} \frac{q\left(R_M-\left\|\mathbf{x}^{(k)}-\mathbf{x}^{(j)}\right\|^2\right)}{2} & \left\|\mathbf{x}^{(k)}-\mathbf{x}^{(j)}\right\| \le R_M \\ \frac{Q}{R_M-\left\|\mathbf{x}^{(k)}-\mathbf{x}^{(j)}\right\|}-\frac{\left\|\mathbf{x}^{(k)}-\mathbf{x}^{(j)}\right\|}{(R_C-R_M)^2}+C & \text{if } R_M \le \left\|\mathbf{x}^{(k)}-\mathbf{x}^{(j)}\right\| \le R_C \\ 0 & \text{otherwise} \end{cases} \quad (7)$$

where q and Q are positive constants, and $C = -\frac{2R_M-R_C}{(R_M-R_C)^2}$ is a smoothing constant.

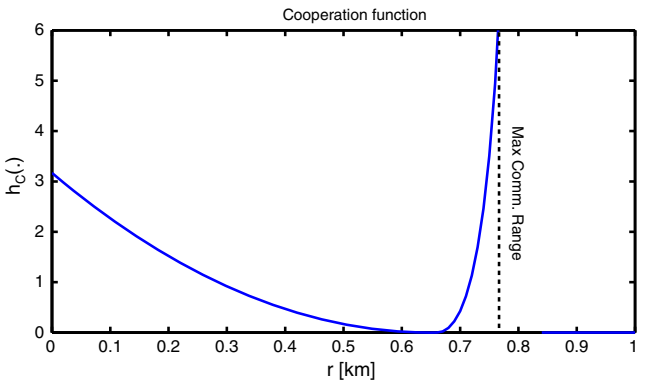

Fig. 5 Interest function for Rule 3: move away from your closest neighbour while maintaining the communication connectivity. The function represents the cohesiveness among the vehicles, as a function of range from the nearest neighbour (move away when the vehicles are close, move closer for values approaching the maximum communication range)

Finally, the agent control input $u(t)$, at each time frame, is obtained as the vector sum of the gradient of each interest function:

$$\mathbf{u}(t) = \mathbf{u}_A(t) + \mathbf{u}_S(t) + \mathbf{u}_C(t) = \nabla h_A + \nabla h_S + \nabla h_C \quad (8)$$

Equation 8 does not guarantee to avoid deadlock situations in which all the vehicles have zero input while the predicted error is still above the desired threshold. While these situations require particular symmetry conditions in the relative positions of the vehicles, and hence are unlikely to occur in practice, there are several ad hoc procedures that can be employed to exit from the deadlock conditions. In particular, we have implemented the following solution: the weight of Rule 1 increases in time if the error condition is not satisfied and the input absolute value is below a pre-set threshold. In this way, the influence of the other vehicles on any given agent decreases with time. Once movement is recovered the deadlock exit rule is abandoned.

The steps in the cooperative adaptive algorithm are now summarized. The algorithm is the same for every vehicle, and it is here described for the jth one.

1. Measurement at point $\mathbf{x}_k^{(j)} : \theta\left(\mathbf{x}_k^{(j)}\right)$
2. Update of the measurement set M_k and the information set I_k with the new measurement and with information made available from the other vehicles
3. Update of the approximated map $S(\mathbf{x})$
4. Choice of the exploration radius
   - 4.1. If the global error (Eq. 3) is below a pre-set threshold, the exploration ends and the algorithm is exited
   - 4.2. If the global error is above the threshold, determine the exploration radius ρ from the current measurement point $\mathbf{x}_k^{(j)}$ as the local fill distance (see Appendix) for which the local error is below the pre-set threshold.
5. Computation of the agent control input:
   - 5.1. Select the closest neighbour, located in $\mathbf{x}^{(k)} \in A$ among all the agents in a range R_C
   - 5.2. Compute the overall velocity control applying Eq. 8 and move accordingly
   - 5.3. Repeat from step 5.1 until $\left\|\mathbf{x}^{(j)}-\mathbf{x}_k^{(j)}\right\|_2 = \rho$ then select $\mathbf{x}_{k+1}^{(j)} = \mathbf{x}^{(j)}$ and repeat from step 1.

Note that the computation of the agent control input is performed at each time frame until a new sampling station is reached at distance p from the last measurement point. For this reason, the selection of the specific point on the frontier of the ball $B\left(\mathbf{x}_k^{(j)},\rho\right)$ depends on the application of the rules while exploring the area. The algorithm does not require any central intelligence, as each agent is able to compute its course independently, on the basis of the shared

knowledge on the past measurements and its closest neighbour location.

Finally, it is worth discussing the communication aspects in the adaptive cooperative algorithm, and in particular those related to step 2 and step 5.

The computation of the approximated map (step 2), which is necessary for each vehicle to compute correctly the exploration radius, requires each agent to share its information on the new measurement executed with all the other agents in the team. This procedure requires networked all-to-all communication and it is the most bandwidth-consuming part of the whole algorithm. However, this operation is only done few times during the exploration and, in particular, only when a new sample is available from one of the members of the team. On the other hand, frequent communication is required during the execution of step 5 of the algorithm, but in this case a very little amount of communication is needed, as each vehicle has to communicate only its current location and only to its closest neighbour.

It is also worth remarking that the cooperative algorithm is robust with respect to sudden or unforeseen change in the communication capabilities (e.g. change in the acoustic propagation, or even faults in the modems) as, in general, it is not required for the vehicles to be connected for the whole mission duration: each vehicle can in any case continue the exploration even though with a decrease in the performance due to the lack of knowledge on the samplings executed by the rest of the team (e.g. samplings too close to each other or not needed). Each agent can always apply Rules 1 and 2 as they only depend on the samplings executed by the connected subset of vehicles.

4 Simulative results

The algorithm testing in simulative scenarios is now reported.

In the following, the same situation of Alvarez et al. (2009) is considered to allow comparisons with other adaptive sampling algorithms even though not completely distributed and based on a strict serial-chain structure, necessary to maintain the communication connectivity.

The objective of the mission is the reconstruction of a salinity field obtained from a restricted access Mediterranean Sea database, on a sub-region 5×5-km width; the data are shown with 100 m×100 m cell resolution (see Fig. 6).

To make it easier to evaluate the algorithm performance, we consider that all the agents move at a constant depth of 50 m when in transit from one sampling station to another, and that they collect data only when they have reached the new sampling

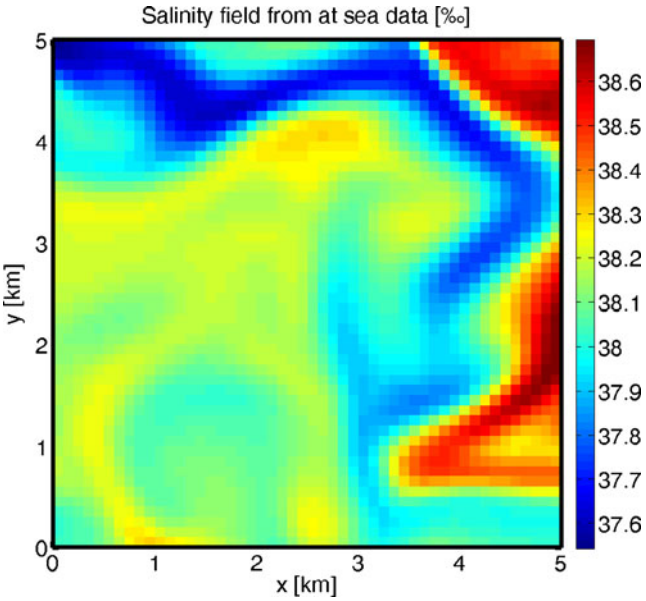

Fig. 6 Salinity field (‰) at 50 m depth, as obtained from at sea data

location. In addition, we suppose that the vehicles can only navigate using dead-reckoning while they are able to localize themselves when on surface and in particular after each sampling measurement. This also implies that the vehicles are not able to take into account the effects of external and unknown disturbances, such as ocean currents, during the navigation phase. In this sense, the adaptive algorithm can only re-act a posteriori, after that the navigation phase is completed and the new measurements have been taken and localized (e.g. vehicles on surface using GPS).

Three cooperating vehicles moving at the maximum speed of 2.5 m/s perform the mission, and each vehicle in the team is equipped with sensors able to measure the salinity field and with a network device that allows communication between any two vehicles in the team if their distance is less than 1 km. For greater distances, and up to 1.5 km, two vehicles can still communicate but with a decrease in performance, in terms of probability of message loss (P_{ml}) proportional to the distance, and in accordance to Eq. 9.

$$\begin{cases} P_{ml}(r) = 0 & if\, r \leq 1km \\ P_{ml}(r) = 1 & if\, r \geq 1.5km \\ P_{ml}(r) = 2r - 2 & otherwise \end{cases} \tag{9}$$

In the first simulation performed, no external disturbances are present, which means that $\mathbf{v} = 0, \forall t, \forall \mathbf{x} \in A$ in Model 4.

Figure 7 shows a sequence of snapshots of the vehicles trajectories during the exploration. The vehicles use the data acquired during the exploration to autonomously select new sampling locations, while adapting the exploration

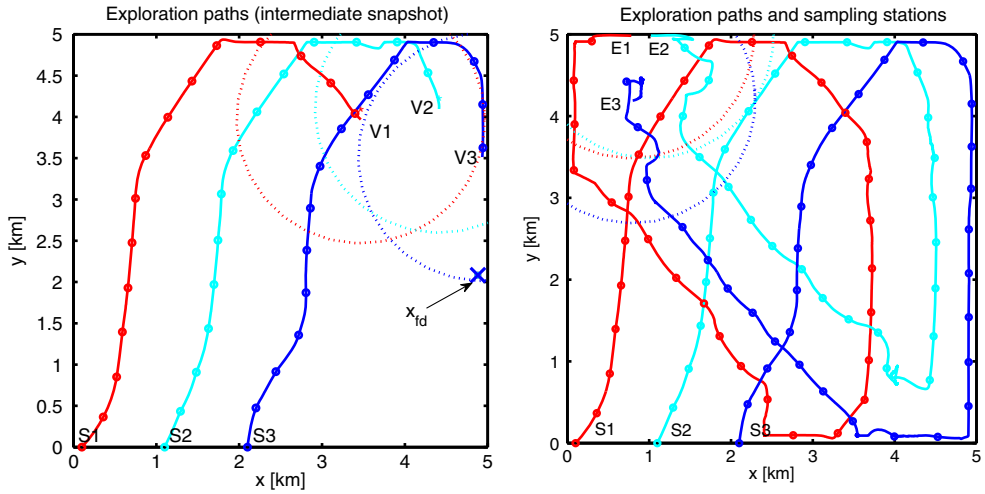

Fig. 7 Snapshots of paths in the mission area during the exploration with a team of three vehicles. Sampling points are represented as circles. A *dashed circumference* represents the maximum communication range of each agent. The vehicles use the data acquired during the mission to driven the exploration autonomously deciding new sampling locations to achieve the desired approximation error at the end of the mission. Note that the artefact on the *cyan line* (vehicle 3) in the bottom-right part of the path is due to the fact that agent 3 is looking for a new sampling location which can respect the imposed constraints (communication constraints, samplings not too close to each other). In this case, the agent is in fact forced to wait for the other two agents to take their samplings while adapting its position in order to maintain the communication. Finally, the whole group move in order to reach the opposite side of the exploration area where the sampling density is lower

radius in order to maintain the approximation error under control. The exploration is completed in 2 h and 54 min, excluding time for samplings acquisition, and the final salinity field reconstructed from 101 samplings using RBF multiquadric approximation is shown in Fig. 8. Comparing the efficiency of the proposed approach with that of the graph-based algorithm in Alvarez et al. (2009), where the number of sampling point is 92, all else being equal, it is seen that our algorithm decreases the efficiency of slightly less than 10%, in this simulative case. We remark that the algorithm proposed here does not rely on explicit knowledge of a cost function to be minimized, and it is solely based on local distributed behaviours.

Finally, Fig. 9 shows the overall approximation error. In particular, in the present simulation case, the maximum

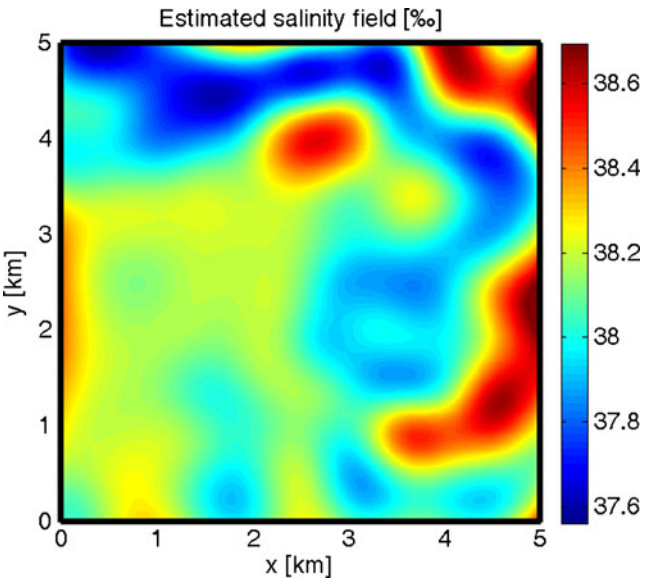

Fig. 8 Salinity field reconstructed from the samplings performed by the cooperative adaptive algorithm using multiquadric RBF approximation

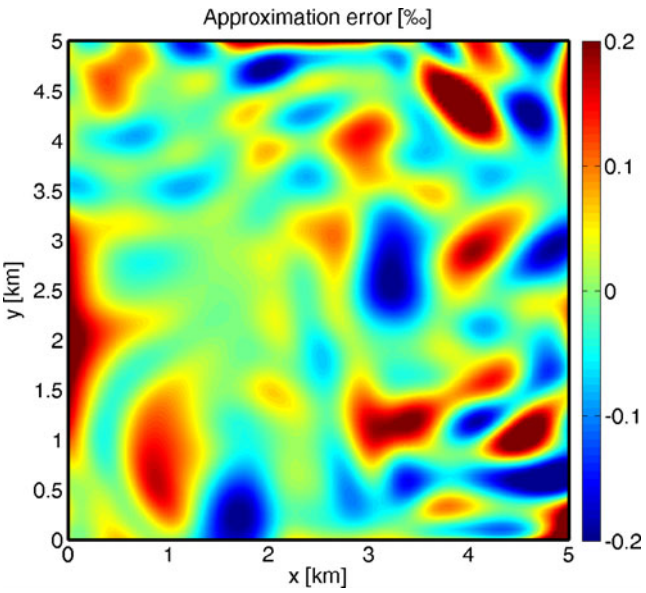

Fig. 9 Approximation error in the exploration area. The mean error absolute value is 0.06‰ while the maximum error, obtained in a very small sub-region at the bottom-right corner of the area, is 0.5‰. To better emphasize the error distribution the maximum error has been saturated from the picture

approximation error in the whole area is $\varepsilon_{\mathrm{Max}} = 0.5‰$. The mean error is $\overline{\varepsilon} = 0.06‰$.

It is worth noticing that the maximum error (saturated in the figure to allow also to evaluate the distribution of errors of smaller magnitude) is only reached in the bottom-right corner of the region while in the rest of the area the error stays always below 0.2‰. Such a big approximation error is due to two complementary effects: by the exploration algorithm which tends to increase the samplings in the under-sampled largest regions of the exploration area which are usually the inner parts; and by an RBF border effect as the RBFs may have divergent tails where less data are available. A possible approach in order to avoid or at least limit the effects described above and to improve the field estimation may be the exploration and sampling of areas slightly bigger than the actual areas of interest.

It is also to be underlined, as a weakness of our method as well as of any point sampling method in which the sample spacing is based on the smoothness of the field as predicted from neighbouring measurements, that very rapid spatial variations may be lost, or poorly reconstructed. One obvious way to cope with this problem is to decrease the accuracy threshold D, when a priori information on rapid spatial variation is available.

The vehicles trajectories depend on the vehicles starting points. In turn, this may affect the distribution and the total number of sampling points at the end of the mission. We have experienced in a number of simulations, not reported here, that the distribution of local errors will be affected by the change in sampling points consequent to different initial conditions, while the average error in the reconstructed field is much less sensitive to the choice of sampling points, as long as these are chosen always following the same rules.

Finally, the same scenario is considered including the effects of marine currents, to compare and verify the adaptive algorithm behaviour in presence of more realistic conditions. The current velocity field in the area of interest is shown in Fig. 10 and it is computed on the basis of the data in the Mediterranean Sea gathered by the "Mediterranean Forecasting System". In Fig. 10, the current magnitude in meters per second is shown by different colours and the arrows indicate the current direction. It is important to note that the presence of currents is not directly considered by the adaptive explorative algorithm, which only reacts a posteriori after that the ocean current has already influenced the vehicle motion (term v in Eq. 4). This results in perturbed trajectories and different sampling locations with respect to the previous case. In addition, as the vehicles tend to separate in order to cover the maximum possible area, they move at a distance that is very close to their maximum communication range R_{C} (i.e. the limit at which $P_{\mathrm{ml}} = 0$). In this situation, the presence of currents may cause a temporary deterioration of the communication performance

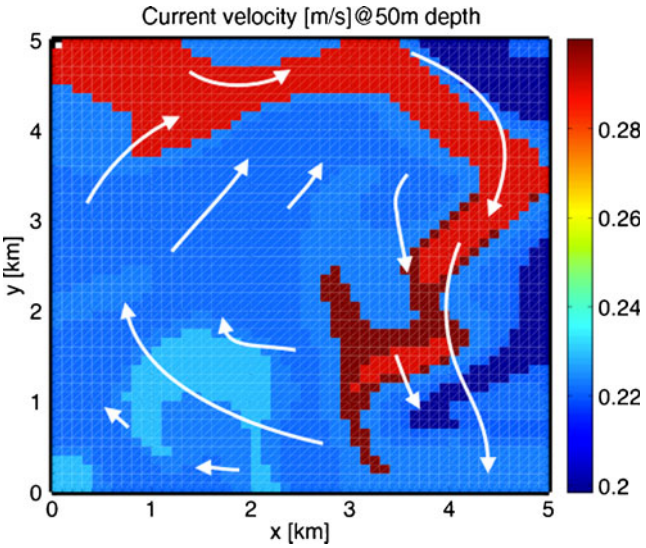

Fig. 10 Current field in the mission area. The *white arrows* indicate the approximate direction of the currents; colours represent the current magnitude in meters per second. Data based on the Mediterranean Forecasting System

forcing the vehicles further than $R_{\mathrm{C}} = 1$ km from their closest neighbours and hence at distances at which the communication is characterized by $P_{\mathrm{ml}} > 0$. In any case, even in presence of currents, the AUVs team is able to cover the entire area (see Fig. 11) in 2 h 33 min (excluding time for sampling acquisition). The mission time has been reduced with respect to the previous case due to the fact that the ocean

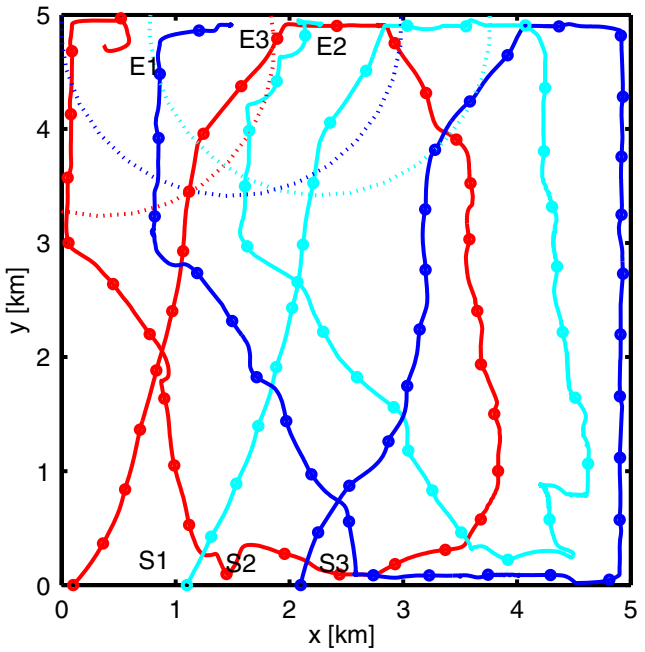

Fig. 11 Exploration paths in presence of currents. For the exploration algorithm currents are simply disturbances and they are not considered directly. This results in perturbed paths for the agents and different sampling locations

current actually increases the speed of the vehicles in certain exploration areas. A slightly larger number of sampling points (107 measurements) is however required to maintain the maximum estimation error under 0.5‰ and the mean error under 0.06‰. The reconstructed salinity field using RBF approximation and the related approximation error are represented in Figs. 12 and 13, respectively.

It is also worth mentioning here that when the current magnitude is very strong, as for example if its order of magnitude is similar or even greater than the nominal speed of the vehicles the exploration becomes quite challenging. In particular, the main effects of a strong current field are twofold:

- It may cause vehicle dispersion if the agents are not able to counteract the ocean current. In this case, a suitable approach should rely on current estimation to produce a control input for the vehicles that is able to compensate, at least partially, the effect of the current. Examples of AUV path planning in presence of currents are given for instance in Alvarez et al. (2004). In any case, even in this scenario, some part of the region may be under-sampled or even totally unexplored.
- The communication connection among the agents cannot be guaranteed resulting in a lack of information during the exploration. This effect is also visible in the case simulated above where the agents move close to their maximum communication range to maximize their coverage of the mission area causing a deterioration of the communication performance. In presence of stronger current fields, this effect will be emphasized, and it must be taken into account to correctly explore the area. Within the setting proposed in this paper, one possible solution may be based on a different shape of the interest functions not to let the agents reach the border of their communication range. Even in this case, however, the maintenance of the communication depends on the current field and cannot be guaranteed a priori.

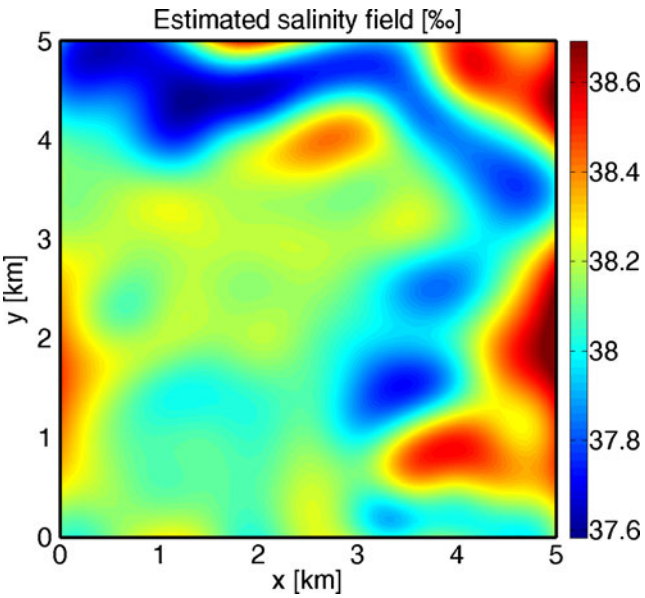

Fig. 12 Salinity field reconstructed using multiquadric RBF approximation from the samplings performed by the cooperative adaptive algorithm in presence of currents

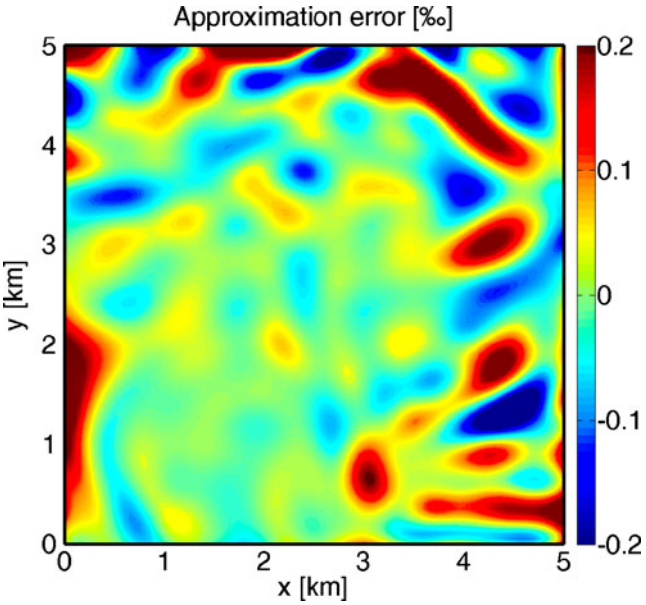

Fig. 13 Approximation error of the salinity field reconstructed on the basis of the measurements performed applying the adaptive cooperative algorithm in presence of marine currents. The maximum error is obtained in the upper border of the exploration area and it is equal to 0.48‰. The mean error is 0.058‰. To better emphasize the error distribution the maximum error has been saturated from the picture

5 Discussion and conclusions

With this paper we have presented a cooperation algorithm for data-driven adaptive sampling of oceanic fields. The main contribution of the proposed approach is in allowing a team of AUVs to autonomously explore an area being driven only by the data as measured during the exploration without need for any central intelligence or supervising authority. The algorithm, based on the idea of emergent behaviours, defines simple rules to characterize each agent behaviour and uses interest functions to prioritize each rule at each time instant, while limiting the amount of communication needed to be exchanged among the team members.

In the paper, we have used the RBF methodology to build incremental approximations of the sampled field and to estimate on-line the smoothness of the oceanic field. Sampling steps are adapted (enlarging or decreasing the

"exploring radius") through the smoothness measure provided by the norm in the native RBF space (see Eq. 3). It is important to remark that the distributed cooperation strategy does not rely on the RBF approach itself. It can indeed be applied without changes also with different methods for field estimation from sparse data, as long as these methods are able to provide on-line an estimate of the local approximation error as a function of the spatial distance between samples.

The algorithm has been designed for the modality of operation in which any AUV measures a depth profile of the environmental quantity of interest at each sampling station; no measurements are taken when vehicles are on transit between sampling locations. This approach is motivated by the fact that in this way the AUV team operation closely resembles traditional oceanographic sampling as conducted from ships; moreover, speed along transit can be increased if the vehicles do not need to simultaneously profile the water column. The class of vehicles described in Alvarez et al. (2009) has been designed to fulfil this operation modality, which implies that navigation from station to station can be done at the water surface, exploiting GPS signals, and resulting in a much simpler and cheaper AUV design. However, there are AUV systems (as the gliders) for which this operation modality is not suited. Typically, a glider measures continuously the oceanic field of interest while yo-yo profiling the water column from one way-point to the next. With this operation modality, it is not required to determine the next "sampling point", but the vehicle trajectory, or track, that maximizes some information-related measure. In this respect, it can be argued that the sampling points of the algorithm described here can also be used as way-points in a glider-like operation, so that the algorithm can be adapted to the gliders case. However, we have not investigated this possibility so far, and it is indeed our opinion that the problem of determining optimal trajectories is richer and wider with respect to the one treated here, and may need a dedicated approach.

One other aspect not addressed in this paper, but that requires dedicated investigation, is that of orienting the survey by tracking specific oceanographic features (gradients, isothermal depths, etc.). This aspect can be considered with the point sampling approach proposed here, or through continuous sampling. In the case of point sampling, feature tracking imposes an additional constraint as for the direction of the next sampling point: in particular, once the exploring radius is determined for a given stage, it is not true anymore that all the points at exploring radius distance are equally feasible points. A privileged direction will be present, and act as an attractor potential field in addition to the other ones related to communication distance, area coverage, distance from already sampled points. Note that, with our rule-based method, strict feature tracking will in general not be possible, since vehicle motion results from summation of different rules and different potential field attractors. If one is interested in following a gradient, or to move along a level curve, direct team formation control should be considered, as in Paley et al. (2008) and Leonard et al. (2010).

A simulative case has been used in order to highlight benefits and drawback of the method. The case has been selected in order to include local variations of salinity up to 0.8‰ at 500 m distance, which we considered a rather challenging situation. The results show that while the vehicle team does indeed behave as expected, data-driven adaptive sampling may miss some of the oceanic field features. The distribution of approximation errors (Figs. 9 and 13) shows that there are location on the mapped area with high errors, notwithstanding the fact that the average error is kept below the desired threshold. Roughly speaking, this situation may happen whenever the estimated local smoothness is such to encourage a sampling step ("exploring radius") such to jump over a relevant variation of the field, hence missing the feature. From an analytic point of view, this situation is discussed in the Appendix (Eqs. 16 and 17 in the Appendix, and discussion thereafter). Clearly, if the oceanic field is smoother than the approximation (condition of Eq. 16 in the Appendix), features will never be missed. However, this condition may very seldom be respected in practice, and it was not respected in our simulative case. We have purposely chosen a field case that poses challenges to our approach, in order to show the drawbacks as well as the potential of the method: a much more homogeneous oceanic field may have produced better looking, though less informative results. Note that a number of ad hoc recipes can be built to mitigate the drawback, all of them based on additional prior knowledge on the field itself. For instance, an upper bound may be imposed on the exploring radius corresponding to the smaller spatial scale one wish to identify. Overall, it is our opinion that even in this challenging case and with no ad hoc solutions, the results obtained, in terms of average approximation error and field feature reconstruction are not to be discarded as useless.

The paper has been concentrated in describing the data-driven approach as a stand-alone system. As pointed out by one of the reviewers of this manuscript, data-driven approaches maybe of interest in mapping unexpected oceanic variability. While model-driven methods provide a guideline to sample the large-scale variability, data-driven techniques have the flexibility to adapt to sample small scale features missed in the ocean models. From this perspective, a hybrid architecture combining model-driven and data-driven sampling may provide an optimized sampling strategy.

Acknowledgements The authors are grateful to the anonymous reviewers for their constructive criticisms and suggestions. This work was supported in part by European Union, 7th Framework Programme, Project UAN—Underwater Acoustic Network under Grant no. 225669 and Project Co^3 AUV—Cognitive Cooperative Control for Autonomous Underwater Vehicles", Grant n. IST-231378.

Appendix A: Exploiting approximation properties of radial basis functions

The development of the approach described in the paper depends on the method employed to estimate the approximation error. In this section, we explain in more detail the approximation algorithms belonging to the class of Radial Basis Function (RBFs) and in particular we focus on how they can be used to derive an analytical formulation of the estimation error.

The reasons, in the present context, for choosing RBFs over other types of approximation methods are several: Radial basis functions, which have a long successful history of applications in the environmental field and in geostatistics (see the classic work of Hardy 1990), are ideally suited for interpolation and approximation of maps sampled on irregular grids (i.e., with samples not necessarily evenly spaced), as it is the case discussed in this paper. Moreover, the RBFs class is still fairly general, including multiquadric functions, thin-plate splines, B-splines, Gaussian functions, etc. The basic results on RBFs employed in the following of the section can be found in Schaback (1995) and (1997).

Let us select a family of RBFs $\Phi : \Re^d \rightarrow \Re$, where d=2 in our case; then the approximation algorithm S becomes:

$$S_{I^{(j)}}(\mathbf{x}) = \sum_{h=1}^{n} \sum_{i=1}^{k_h} \alpha_{h,j} \Phi\left(\mathbf{x} - \mathbf{x}_{h,j}\right) \tag{10}$$

In Eq. 10, it is assumed that one basis function is centred at each sampled point: strictly speaking, this means that we are performing an interpolation of the measured data, and not an approximation. This assumption, which in some condition may lead to numerical difficulties, does not affect the generality of the discussion and it can be relaxed using approximation formulas (see Caiti et al. (2007), Iske (2003)).

Let $\theta : \Re^d \rightarrow \Re$ be the true function approximated by S. It is assumed that $\theta(\mathbf{x})$ has Fourier transform $\theta(\omega)$, satisfying the following smoothness condition:

$$\frac{\overline{\theta}(\omega)}{\sqrt{\overline{\Phi}(\omega)}} \in L_2\left(\Re^d\right) \tag{11}$$

where $\overline{\Phi}$ is the generalized Fourier transform of the chosen RBF. Then θ belongs to a space H which has the structure of a Hilbert space with $\Phi(\mathbf{x}, \mathbf{y})$ as reproducing kernel, and (semi-)norm:

$$\|\theta\|_{\Phi}^2 = (2\pi)^{-d} \int_{\Re^d} \frac{\left|\theta(\omega)\right|^2}{\Phi(\omega)} d\omega \tag{12}$$

Note that the assumption of θ belonging to a specific reproducing kernel Hilbert space is an assumption on the regularity of the environmental map with respect to (x, y) coordinates. Note also that, depending on the specific choice amongst the RBF family, Φ can be positive definite, hence equation (12) is a norm, or conditionally positive definite, hence equation (12) is a semi-norm. If Φ is conditionally positive definite (of order m) the interpolation equation (10) must be complemented with a polynomial of degree m taking null values in the measured point and spanning the set of functions P_m. The Hilbert space is then $H \backslash P_m$. In both cases the interpolation formulas reported in the following do not change, and the difference between the practical implications of the two cases is negligible.

Within this setting, the approximation error in a ball of radius ρ centred in a point x is given by:

$$\varepsilon(\mathbf{x}) = |\theta(\mathbf{x}) - S(\mathbf{x})| \leq \|\theta\|_{\Phi} F_{\Phi}\left(h_{\rho}\right) \tag{13}$$

where the explicit dependence of ε and S from the information set I has been omitted for the sake of simplicity. The quantity h_p is the so-called *local fill distance*, in the RBFs jargon, and it depends on the density of the sampling points:

$$h_{\rho}(y) = \sup_{w \in B(y,\rho)} \min_{\mathbf{x} \in M^{(j)}} \|w - \mathbf{x}\|_2 \tag{14}$$

while $F_{\Phi}()$ (the *power function*) is a known function that depends exclusively on the specific RBF choice (gaussian, multiquadric, etc.); some typical forms, given by Schaback (1995), are reported in Table 1. Under some additional technical assumptions - decay to zero of the RBF Fourier transform, and uniform interior cone condition holding on the domain of interest A (Iske (2003))—Eq. (13) can be extended

Table 1 Expression of the bounds on the power function (Eq. 13) as a function of the RBF family chosen (from Schaback 1995)

Radial basis function	Bound of power function: $F_{\phi}(h)$
Thin-plate spline $\phi(r) = r^{\beta} \log(r)$	$h^{\beta}/_2$
Multiquadrics $\phi(r) = \sqrt{(r^2 + c^2)}$	$e^{-\frac{\delta}{h}}, \delta > 0$
Gaussian $\phi(r) = e^{-r^2}$	$e^{-\frac{\delta}{h^2}}, \delta > 0$
Inverse multiquadrics $\phi(r) = (r^2 + c)^{-\frac{1}{2}}$	$e^{-\frac{\delta}{h}}, \delta > 0$

to the whole domain A by replacing the local fill distance with the *global fill distance*:

$$h_{A,M^{(j)}}(y) = \sup_{w\in A}\min_{\mathbf{x}\in M^{(j)}} \|w-\mathbf{x}\|_2 \tag{15}$$

Note that the technical assumptions for the existence of a global fill distance are respected by the RBFs of Table 1, and that a compact, convex domain A is sufficient to guarantee the interior cone condition.

As evident, the approximation error in Eq. 13 depends on the unknown norm of the true $\|\theta\|_\Phi$ and cannot be evaluated from the data; however, by assuming that the following condition holds:

$$\frac{\overline{\theta}(\omega)}{\sqrt{\overline{\Phi}(\omega)}} \le \frac{\overline{S}(\omega)}{\sqrt{\overline{\Phi}(\omega)}} \tag{16}$$

the following bound holds true (see Schaback (1995) for a proof):

$$\varepsilon(\mathbf{x}) = |\theta(\mathbf{x}) - S(\mathbf{x})| \le \|S(\mathbf{x})\|_\Phi F_\Phi\big(h_\rho(\mathbf{x})\big) \tag{17}$$

The error bound can now be incrementally computed with the available data using the current approximation of the environmental map at the place of the map itself.

It is worth noticing that, crucial to this development, is the assumption of Eq. 16, which, in practical terms, implies that the environmental map θ is smoother than its approximation S. This regularity condition is indeed much stronger than the assumption of Eq. 12, and it may be more difficult to guarantee a priori. Nevertheless, Eq. 17 can always be used as an approximation of Eq. 13, since as the number of sampling points increase the two expression will eventually converge; however, the bound on the approximation error is not strictly guaranteed anymore at each new sampling stage of the algorithm, causing possibly repeated explorations of the same sub-areas.

Assuming Eq. 16) to hold, the jth vehicle can incrementally determine the radius $p_{k+1}^{(j)}$ at each new step in the planning as the local fill distance to be inserted in Eq. 17 to satisfy the error requirements of the mission.

References

Alvarez A, Caffaz A, Caiti A, Casalino G, Gualdesi L, Turetta A, Viviani R (2009) Fòlaga: a low-cost autonomous underwater vehicle combining glider and AUV capabilities. Ocean Eng 36 (1):24–38

Anderson B, and Crowell J (2005) Workhorse AUV – A cost-sensible new Autonomous Underwater Vehicle for Surveys/Soundings, Search & Rescue, and Research, In Proc. IEEE Oceans'05 Conference

Caiti A, Munafò A, Viviani R (2007) Adaptive on-line planning of environmental sampling missions with a team of cooperating autonomous underwater vehicles. Int J Control 80(7):1151–1168

Caiti A, Crisostomi E, Munafò A (2009) "Physical characterization of acoustic communication channel properties in underwater mobile sensor networks", *Underwater Mobile Sensor Networks* Sensors Systems and Software, Springer Berlin, ISBN978-3-642-11527-1, pp. 121–126

Curtin TB, Bellingham J (2009) "Progress toward autonomous ocean sampling networks", Deep Sea Research Part II. Topic stud Oceanogr 56(3–5):62–67

Curtin T, Bellingham J, Catopovic J, Webb D (1993) Autonomous oceanographic sampling networks. Oceanography 6(3):86–94

Leonard NE, Paley DA, Lekien F, Sepulchre R, Fratantoni DM, Davies RE (2007) Collective motions, sensor networks and ocean sampling. Proc IEEE 95(1):48–74

Leonard NE, Paley DA, Davis RE, Fratantoni DM, Lekien F, Zhang F (2010) Coordinated control of an underwater glider fleet in an adaptive ocean sampling field experiment in Monterey Bay. Int J Field Robot 27(6):718–740

Martinez S, Cortez J, Bullo F (2007) "Motion coordination with distributed information", IEEE Control System Magazine, pp. 75–88, August 2007

Mediterranean forecasting system towards environmental predictions, available online at: mfstep.bo.ingv.it. Accessed by January 15, 2011.

Paley DA, Zhang F, Leonard NE (2008) Cooperative control for ocean sampling: the glider coordinated control system. IEEE Trans Control Syst Technol 16(4):735–744

Schaback R (1997) "Reconstruction of multivariate functions from scattered data", available on line at: http://www.num.math.uni-goettingen.de/schaback/research/group.html. Accessed by April 5, 2011.

Tanner HG, Jabadaie A, Pappas GJ (2003) "Stable flocking of mobile agents, part I: fixed topology", Proc. 42nd IEEE Conference on Decisions and Control

Yilmaz NK, Evangelinos C, Lermusiaux PFJ, Patrikalakis NM (2008) Path planning of autonomous underwater vehicles for adaptive sampling using mixed integer linear programming. IEEE J Ocean Eng 33(4):522–536

Schaback R (1995) "Multivariate interpolation and approximation by translates of a radial basis function", *Approximation Theory VIII* C.K.Chui, L. L. Schumaker (eds.), World Scientific Publishing Co., 1995

Iske A (2003) "Radial basis function: basics, advanced topics and meshfree methods for transport problem", *Spline and radial basis function*, vol. 61, n. 3, Rend. Sem. Mat. Univ. Pol. Torino, Italy, 2003

Alvarez A, Caiti A, Onken R (2004) Evolutionary path planning for autonomous underwater vehicles in a variable ocean. IEEE J Ocean Eng 29:418–429, n.2